RESEARCH ARTICLE

OPEN ACCESS

Optimizing Low-grade Astrocytoma Radiotherapy Dose Prediction through Image-based Discriminative Models

Pooya Mazloomi[1] [ID], Niloufar Naddafi[1] [ID], Toktam Khatibi[1,*] [ID] and Abdolazim Sedighipashki[2]

[1]*School of Industrial and Systems Engineering, Tarbiat Modares University (TMU), Tehran, 14117-13114, Iran*
[2]*Department of Radio Oncology, School of Medicine Cancer Research Center, Hamedan University of Medical Sciences, Hamadan, Iran*

Abstract:

Introduction: Low-grade astrocytomas are common, slow-growing tumors that can progress to high-grade forms if treatment is unsuccessful, with an average survival of 4.7 to 9.8 years. Five-year survival is 80% for low-grade but under 5% for high-grade with all grades proving invasive and treatment-resistant. Post-surgery radiotherapy, requiring precise dosing to protect healthy cells, is key for efficacy and minimal side effects. This research predicts the best dose of radiation therapy for patients with astrocytoma based on the analysis of images of brain patients and discriminative models. Data related to 33 patients were collected from the Mahdieh Radiation Oncology Department. These data included 2745 MRI images of subjects suffering from low-grade astrocytoma (axial, sagittal and coronal views) with a resolution of 512 × 512 pixels, along with the clinical characteristics and treatment characteristics of the patients.

Methods: In this research, two problems of regression and classification were examined. The purpose of the regression problem is to simultaneously estimate the patient's radiotherapy sessions and their corresponding dosage, and in the classification problem, the purpose of the classification problem is to classify patients into 4 classes according to the amount of prescribed dose using past data. By combining the VIT model and the CNN network, a powerful feature extraction model from images was designed, and then regression and classification problems were solved with the help of the MLP network and SVM and Random Forest algorithms.

Results: The best results were related to the CNN_VIT-b16 model, which was able to predict the number of radiotherapy sessions with a mean absolute error of 0.005 and an R^2 score of 0.993 in the problem of predicting the prescribed dose of radiotherapy with the mean absolute error of 0.0034 and an R^2 score of 0.998. Moreover, in the classification problem, it achieves 0.99 accuracy and 0.99 F1 score on the test data.

Discussion: This study demonstrated that a hybrid CNN-ViT model could accurately predict radiotherapy dosage and session counts for low-grade astrocytoma patients using MRI images and clinical data, achieving near-perfect regression and classification performance. The model's strong results suggest it could serve as an effective decision-support tool to personalize treatment and reduce harm to healthy tissue. Despite the promising outcomes, validation on larger, more diverse datasets is needed before clinical deployment.

Conclusion: This research designed a diagnostic-aided model that predicts the radiotherapy plan for treating patients with astrocytoma. The radiotherapy dose and number of sessions are tailored to the individual, varying with tumor size, type, and the patient's overall health, thus complicating treatment planning. A model designed to consider these factors could aid doctors in diagnosing and treating low-grade astrocytoma. Such a model could serve as a valuable diagnostic support tool.

Keywords: Brain tumor, Image processing, Feature extraction, Artificial intelligence, Diagnostic assistance system.

*Address correspondence to this author at the School of Industrial and Systems Engineering, Tarbiat Modares University (TMU), Tehran, 14117-13114, Iran; Tel: 982182883913; E-mail: toktam.khatibi@modares.ac.ir

1. INTRODUCTION

Astrocytomas, originating within the brain itself, pose a considerable threat due to the complexities involved in both identifying and managing them. Slower-growing, lower-grade astrocytomas represent a prevalent type of brain tumor, with the potential to evolve into more aggressive, higher-grade forms if interventions prove unsuccessful [1]. Aligned with the World Health Organization's 2016 categorization of central nervous system tumors, astrocytomas are distinguished as either low-grade (LGA, WHO II) or anaplastic (AA, or high-grade, WHO III), each requiring distinct treatment approaches and exhibiting varying prognoses [2]. Low-grade astrocytomas are infiltrative brain tumors that stem from glial cells, often emerging unexpectedly in young or middle-aged individuals. Their expansion rate is typically more gradual compared to higher-grade variants. Representing 10-20% of primary brain tumors, low-grade astrocytomas constitute a noteworthy subset of these conditions [3].

The patient's initial symptoms and imaging results are key factors in guiding the management of astrocytoma [4]. Seizures are the most common symptom of the disease, which occurs in 80% of patients. Other common symptoms include headaches, sluggishness, fatigue, and variations in personality. For some other patients, disease detection may be postponed due to the tumor's slow growth rate. Surgical intervention is often required when symptoms arise from mass effect or increased intracranial pressure. However, managing patients who show no tumor growth on imaging and whose symptoms are effectively managed with medication presents a greater challenge and elicits debate [5, 6].

Survival rates for astrocytoma vary widely depending on the tumor's grade, location, size, and the patient's age and overall health, ranging from approximately 4.7 to 10 years [7]. The 5-year survival rates for low and high grades of astrocytoma are about 80 and less than 5%, respectively. Regardless of tumor grade, astrocytomas are highly infiltrative and resistant to treatment, thus becoming largely incurable [8].

While the query provides an estimate of 2,000 to 3,000 low-grade astrocytoma diagnoses per year, a 2017 estimate reported 1,410 new cases of diffuse astrocytoma in the United States5. Low-grade astrocytomas account for 10-20% of primary brain tumors1. Low-grade astrocytomas are predominant in individuals aged 30 to 40, comprising about one-fourth of adult cases. The peak incidence of astrocytomas generally occurs in people aged 35 to 44 years, and they are more frequently observed in white individuals and males. Identifying factors impacting survival in astrocytoma patients remains a crucial area of investigation [9].

The best treatment methods include surgery and tumor removal, radiation therapy and chemotherapy [9]. Radiotherapy is one of the essential ways to deal with and treat all types of brain tumors. Radiotherapy is effective in controlling tumor growth and excessive hormone secretion in patients with pituitary adenoma.

For tumors like optic tract glioma, radiotherapy—used alone or with surgery/chemo—achieves 70-95% long-term control. Protocols specify total dose (50-60 Gy), section dose (2-1.8 Gy), and treatment days (5/week). Normal brain structures are sensitive to these parameters, affecting late effects. 3D conformal radiotherapy, where beams conform to the tumor's shape, is the standard CRT method [10].

During the previous years, different medical imaging techniques have been exploited for disease diagnosis [11]. However, with emerging novel imaging techniques, radiologists encounter a growing amount of data for detecting diseases and planning patient treatment. Therefore, it becomes necessary to use automatic and intelligent systems in such matters.

Deep neural networks (deep learning) are the emerging trend of machine learning models with a high popularity for medical image analysis. End-to-end models for performing both tasks of feature extraction and prediction simultaneously have been used instead of handcrafted feature extraction to reduce the dependency of data scientists on domain knowledge for feature extraction and prediction tasks while providing high accuracy for automatic diagnosis and treatment designing [12]. Machine learning, particularly deep learning, has been widely applied in various medical image analysis tasks [13].

There are three fundamental limitations of existing approaches including:

1.1. Overcoming Isolated Feature Analysis in Conventional Models

Current CNN-based methods focus exclusively on local tumor morphology from MRI slices, while clinical systems often rely on manual geometric measurements of tumor boundaries. Our dual-stream architecture directly integrates:

a-1) Local texture analysis *via* ResNet-34 (processing 128×128 MRI patches).

a_2) Global spatial relationships through ViT-b16's self-attention across whole-image regions.

We hope this combination will reduce dose prediction errors compared to ViT-only implementations in ablation studies, demonstrating superior modeling of tumor-structure interactions critical for dose planning.

1.2. Bridging the Multimodal Integration Gap

Traditional clinical workflows process imaging and patient data separately, while prior computational models use simplistic early fusion (concatenating features). Our model introduces:

b-1) Dynamic attention gates that weight MRI features against clinical parameters (age, tumor volume, surgery history)

b-2) Joint optimization of radiation dose and session count through parallel MLP heads

We hope this architecture will achieve a higher R^2 score compared to early fusion baselines by preventing clinical data dominance over imaging features.

1.3. Addressing Clinical Validation Shortcomings

Existing computational studies primarily report technical metrics like MAE, while clinical systems lack quantitative validation frameworks.

2. BACKGROUND

Novel deep learning models have significantly impacted medical image analysis and offer promising applications in medical fields, including brain cancer. This section reviews relevant research proposing and using deep learning methods for the diagnosis of brain tumors from MRI images. While the studies reviewed here do not directly focus on predicting the dose required by patients, they demonstrate the ability of neural networks for various tasks for brain cancer diagnosis.

2.1. Brain Tumor Classification

Diagnosing brain tumor types and grades is an interesting research area based on its importance and necessity. In a study, two classification models, SVM and Lasso, were used to classify high-grade and low-grade glioma tumors, utilizing pre-processed MR images along with tumor location and size. The feature extraction method used in this research was based on region of interest (ROI) analysis [14]. In another study, some pretrained neural networks were exploited and compared for the discrimination of brain tumor types, including glioma, meningioma, and pituitary, by examining MR images from a publicly available research dataset [15]. Also, in another study, a completely automatic method was presented for segmenting MRI images and determining tumor types, including meningioma, glioma, and pituitary tumors, using a deep neural network [16].

Most previous studies have designed and used Convolutional Neural Networks (CNNs) from scratch or used pretrained CNNs for MRI image analysis. However, numerous deep neural networks have been proposed in recent years, including Recurrent Neural Networks (RNNs), Autoencoders (AEs) [17], and Vision Transformers, which utilize self-attention mechanisms and support parallel processing for feature extraction [18].

In 2019, the vision transformer was introduced by a study [19]. The goal of this new approach is to process images without relying on traditional convolutional operations commonly used in computer vision tasks. While self-attention mechanisms in transformers were originally designed to capture relationships between words in the text, Vision Transformers have extended this concept to computer vision and image processing. The key idea behind the vision transformer was to first divide the input images into a set of patches, which are then transformed into vectors. These vector representations are treated like "words" in a typical transformer and allow the model to capture the relationships between different pieces of an image. Today, the performance of a transformer model is surpassing convolutional neural networks (CNN) in image classification tasks. In a 2024 study, he compared the performance of CNN and VIT networks on x-ray images of patients with COVID-19 [20]. The impact of the vision transformer has extended beyond the confines of research labs and into real-world applications. The combination of VIT networks with CNN networks has brought about significant advances in the field of medicine [21].

2.2. Deep Neural Networks and Transformers Applications

Recent years have witnessed a surge in the application of deep learning, particularly transformer-based models, for diverse medical image analysis tasks. For instance, in the domain of neurological disorders, researchers have explored the use of dual-patch attention mechanisms for epileptic seizure prediction [22-24] and mixed transformer architectures for the early diagnosis of multi-class Alzheimer's disease [25]. Furthermore, the effective diagnosis of acute bilirubin encephalopathy through multi-modal neonatal Magnetic Resonance Imaging has been achieved using multi-transformer networks, highlighting the capability of these models to integrate information from different imaging modalities [26]. These studies demonstrate the increasing trend towards employing sophisticated deep-learning architectures to tackle complex diagnostic challenges in medicine.

Beyond diagnostic accuracy, the interpretability and robustness of deep learning models are gaining increasing attention. Explainable AI (XAI) frameworks are being developed to provide insights into the decision-making processes of these models, as exemplified by the use of relevance-aware capsule networks for breast cancer detection in mammography images [27]. Additionally, the evaluation of model dependence on data complexity is crucial for ensuring reliable performance across diverse datasets. Studies focusing on brain MRI images have explored the relationship between data complexity and model performance in the classification of brain tumors and Alzheimer's disease [28]. These advancements underscore the importance of not only achieving high accuracy but also ensuring the transparency and generalizability of deep learning models in medical image analysis.

3. MATERIALS AND METHODS

3.1. Dataset

In this study, brain MRI images of patients with low-grade astrocytoma were collected from Mahdieh Imaging and Radiology Center located in Hamedan, Iran. Since this study required the collection and integration of various datasets, including MRI images, clinical data, and patients' medical histories, these datasets were obtained separately. Therefore, only patients with complete and accessible information were included in the analysis.

Thirty-three patients were examined in this center and 2745 MRI images were extracted in 3 directions in DICOM format from the PACS system of Mahdieh center, which can be seen in Fig. (1). In addition to these images, other demographic information about the patients was also reviewed, including gender, age, disease symptoms, history of surgery before radiation therapy, and details of the patients' radiology sessions, such as the number of radiotherapy sessions, the dose used in each session, and the total dose administered during the course of treatment. The medical and radiotherapy files of the patients were collected. Finally, the data collected from the patient's files were tabulated and saved in an Excel file. Patients suffering from low-grade astrocytoma were confirmed by the pathology reports of the patients and the treatment method prescribed for each patient by the specialist doctor of the center.

The sample size in this study was determined by the availability of complete and well-documented patient data at the Mahdieh Radiation Oncology Department during the study period. Collecting comprehensive data, including MRI images, clinical characteristics, and detailed treatment records, is a time-consuming and resource-intensive process. We aimed to maximize the number of patients included while ensuring the integrity and completeness of the data. Given the retrospective nature of our study and the challenges associated with data collection, we believe that the 33 patients represent a valuable initial dataset for exploring the feasibility of using deep learning models for astrocytoma radiotherapy dose prediction.

We acknowledge that this sample size may limit the generalizability of our findings and the statistical power of our analyses. The best way to mitigate the limited sample size is to implement a stratified 5-fold cross-validation strategy, ensuring each fold maintains the original class distribution.

3.2. Preprocessing

MRI images were collected in DICOM format from the PACS system. First, the images were converted from DICOM (Digital Imaging and Communications in Medicine) format to JPG format with a resolution of 512 x 512 pixels for easier access and display and processing by the model. DICOM is a format of medical imaging standard [23].

In the next step, the textual information inside the images was removed to reduce the error in the neural network model. Finally, due to the high volume of images and with the aim of reducing computing costs, the resolution of the images was changed to 128 x 128 pixels.

We reduced the image resolution to 128x128 pixels primarily to manage computational costs and memory requirements, given the large number of images (2745) and limited computational resources. This resolution was chosen as a trade-off between computational efficiency and the preservation of essential tumor features.

Also, the image pixels were normalized to a range between 0 and 1 after loading the model. The required columns of tabular data were also pre-processed by the One-hot-encoding method to remove the sequential effect in the classification problem.

3.3. Define Problem

In this research, the two problems of regression and classification were investigated simultaneously by a model designed with multiple outputs. In the regression problem, the goal of the model is to accurately and simultaneously predict the best prescription dose along with the number of sessions required for each patient according to past data. In the classification problem, first, the prescribed dosage range for each patient was specified and then this range was divided into 4 classes. Thus, patients with a prescribed dose of less than 5000 were placed in class 1, between 5001 and
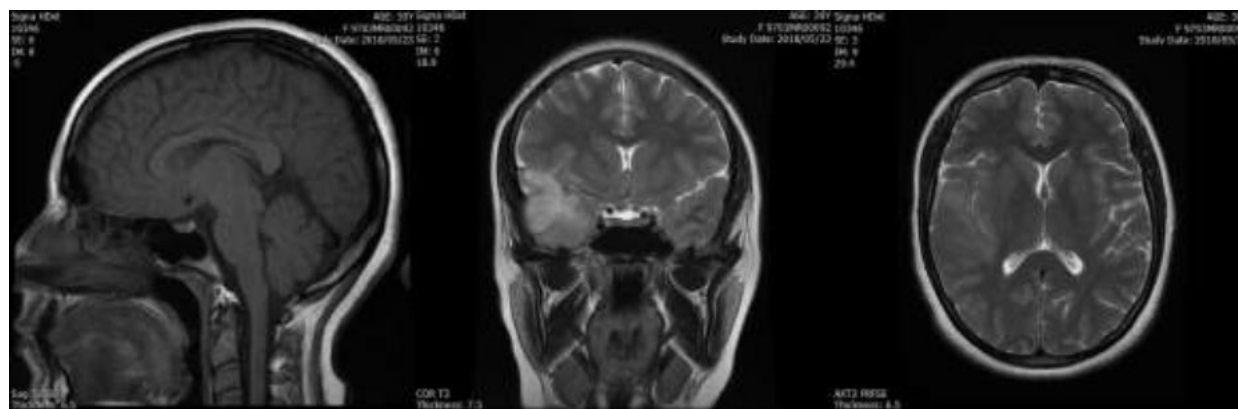
Fig. (1). An example of MRI images of patients in four different views: left, posterior, and superior, from left to right.

5500 in class 2, between 5501 and 6000 in class 3, and above 6001 in class 4. 2D CNN model and Vision Transformer-b16 and Vision Transformer-b32 networks were used for feature extraction. Machine learning and neural network algorithms were used in the models designed for the classification problem. In the following sections, we will examine the architecture of the top models according to the selected data.

3.4. CNN-VIT-b16

In this model, two inputs were considered: tabular data and MRI images. To extract features from the MRI images, they are fed into a VIT-b16 network and a CNN in parallel. For the VIT-b16 network, the linear classification layer and softmax, responsible for data classification, were removed to repurpose it for feature extraction. After feature extraction from the VIT-b16 network, a Flatten layer was applied to flatten the data. The CNN branch consisted of three convolutional layers with 16, 32, and 64 kernels, respectively, each using a 3x3 kernel size.

After each convolutional layer, a Max pooling layer was used to reduce the dimensions. Subsequently, another convolutional layer with 64 filters was applied, followed by another Max pooling layer to increase data depth. Before combining with tabular data, the flattened outputs from the VIT-b16 network and the CNN were merged into a single feature matrix using a Flatten layer.

The tabular data was processed separately through four dense layers (64, 64, 128, and 128 neurons). The output of the dense layers and the feature matrix from the images were then merged and fed into three dense layers with 512 neurons each.

Finally, the model produced three outputs: one for predicting the number of radiation therapy sessions (regression), one for predicting the total radiation therapy dose (regression), and one for classifying the patient into one of the four dosage classes (classification).

For the regression outputs, a single neuron without an activation function was used. For the classification output, four neurons with a Softmax activation function were used for the four-class classification. All other layers employed the ReLU activation function. ViT is particularly well-suited for this task because, unlike CNNs, which primarily capture local features, ViTs leverage a self-attention mechanism to model long-range dependencies within the entire MRI image, allowing the model to consider the relationships between the tumor and distant critical structures like the optic chiasm or brainstem, which is crucial for precise dose prediction and sparing healthy tissue during radiotherapy planning; furthermore, ViTs can handle the high-resolution images typical in medical imaging without the computational limitations of some other architectures.

ViT-b16 and ViT-b32 refer to Vision Transformer models (Dosovitskiy *et al.*, 2020) with different configurations. The 'ViT' component utilizes a transformer-based architecture to capture long-range dependencies within the MRI images, while 'b16' and 'b32' denote specific model configurations with a base architecture and 16 or 32 transformer blocks, respectively, influencing the model's capacity and computational complexity.

3.5. SVM_RF_VIT-b16

In the proposed model, SVM-RF-VIT, similar to CNN-VIT-b16 architecture, was used in feature extraction from VIT and CNN networks. In other words, VIT and CNN are used as models that extract features from input MRI images. In this model, the default support vector machine (SVM), which is a linear SVM, was used in the regression problem and the random forest (RF) algorithm with N = 97 was used in the classification problem. The feature embeddings extracted using VIT and CNN are concatenated and fed to SVM and RF as their input.

3.6. VIT-b32

In order to compare the two models of VIT-b16 and VIT-b32, all models with VIT-b32 were also examined.

3.7. Train Model

A 5-fold cross-validation sampling strategy is used for splitting data into training and test datasets. Also, 20% of training data as the validation data is sampled from the training dataset.

The hyperparameters were tuned using the Grid Search method. Optimizer, batch size and learning rate and number of epochs are considered hyperparameters. According to the values obtained as the best hyperparameters' value, the designed models were trained with a batch size = 64 and epochs = 100 with a learning rate of 0.001 and a reduction rate of 98% with the aim of reducing fluctuations during training. Adam was used as the optimizer function.

The cost function and evaluation criteria during model training can also be seen in Table **1**.

Table 1. Classification and regression model loss function and metric.

Classification	Regression
Loss function: MAE Metric: MAE	Loss function: Categorical_CrossEntropy Metric: Accuracy

4. RESULTS

The experimental results are described in three parts. Predicting the number of radiation therapy sessions for each patient, predicting the dose of radiation therapy for each patient and classifying patients into 4 classes. In the CNN-VIT-b16 model, the model achieved 99% accuracy in the classification problem and R^2 score of 99.3% in predicting the number of radiotherapy sessions and an R^2 score of 99.8% in predicting the number of prescribed dose sessions for each patient.

The high R^2 values indeed warrant careful consideration. To address this, we implemented several regularization techniques:

L2 Regularization: We applied L2 regularization to the weights of the MLP layers, with a regularization strength (lambda) of 0.001, to prevent the model from relying too heavily on any single feature.

Dropout: We incorporated dropout layers with a rate of 0.5 after each fully connected layer in the MLP. This helps to

prevent co-adaptation of neurons and further reduces overfitting.

Early Stopping: During training, we monitored the validation loss and implemented early stopping to prevent the model from overfitting to the training data. The training process was halted if the validation loss did not improve for 10 epochs.
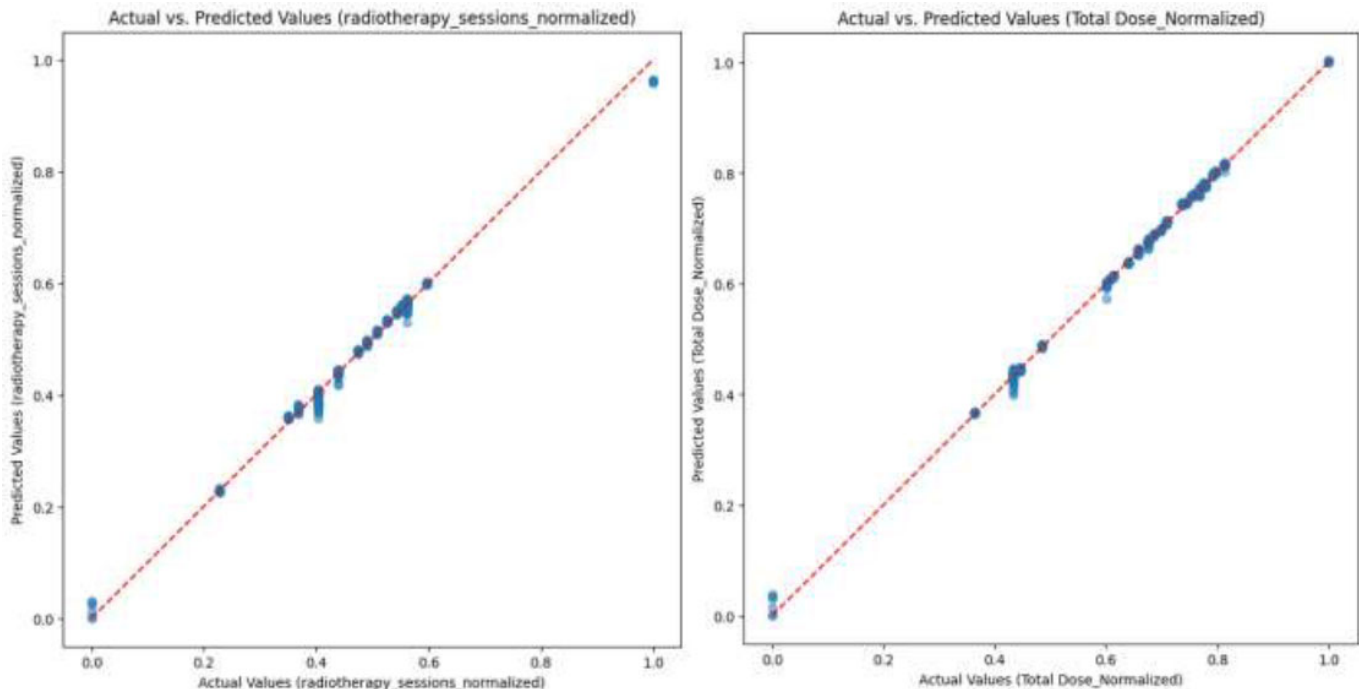
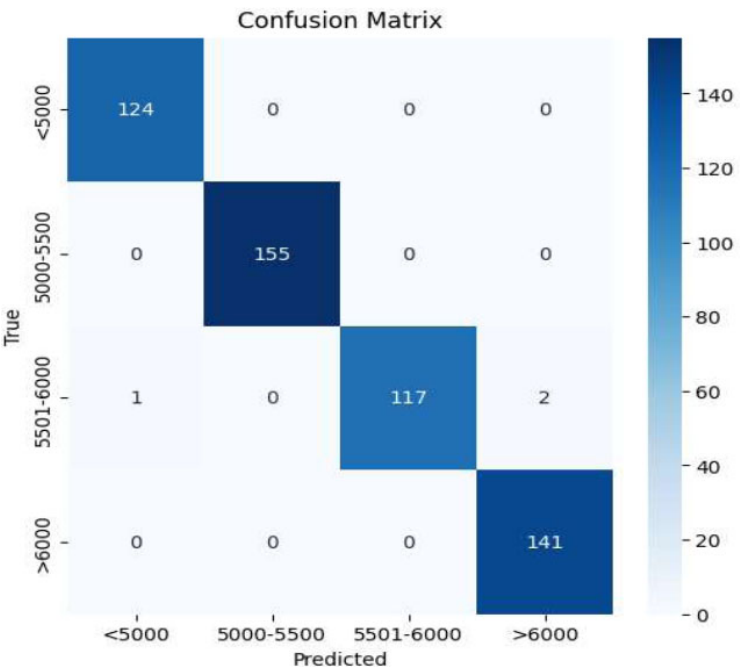The details of the CNN-VIT-b16 model results are displayed in Figs. (2-6).
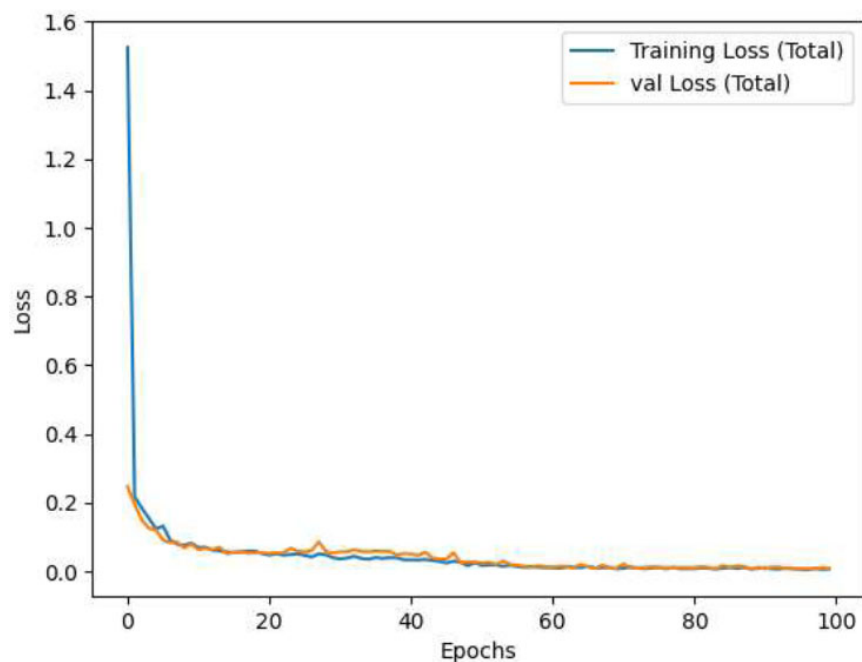
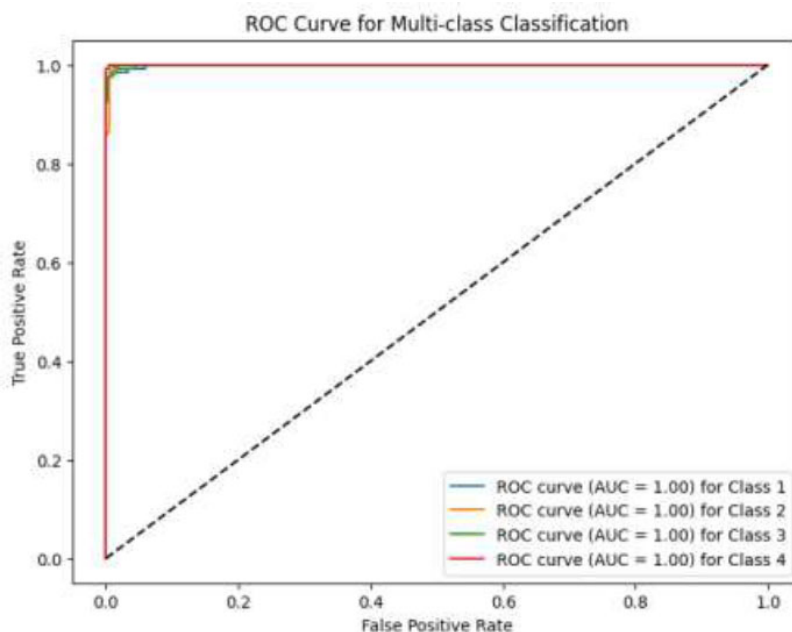**Fig. (2).** CNN-VIT-b16 loss per epochs.
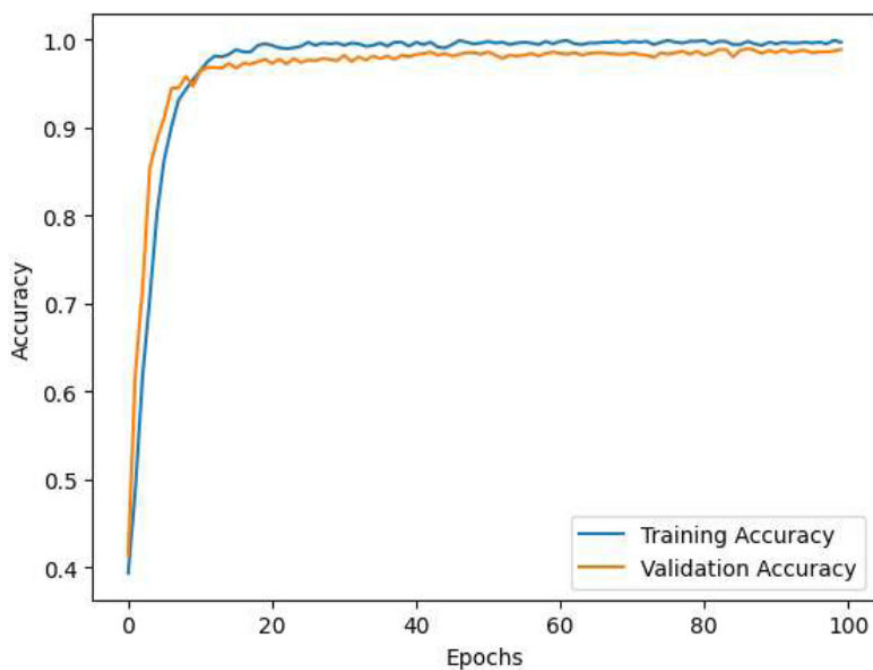
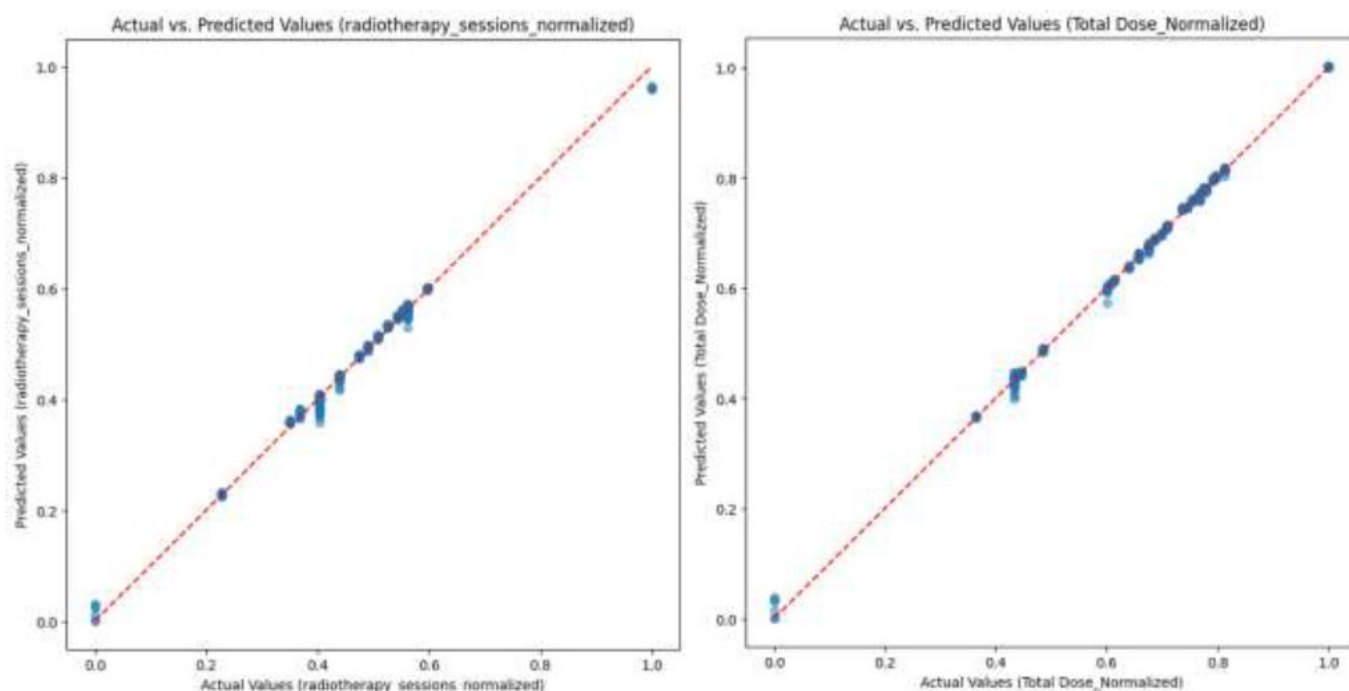**Fig. (3).** CNN-VIT-b16 accuracy per epochs.

Fig. (4). Comparison of predicted values of CNN-VIT-b16 model with actual values for (**a**) normalized number of the radiotherapy sessions and (**b**) normalized total dose.

Fig. (5). Confusion Matrix of CNN-VIT-b16 model
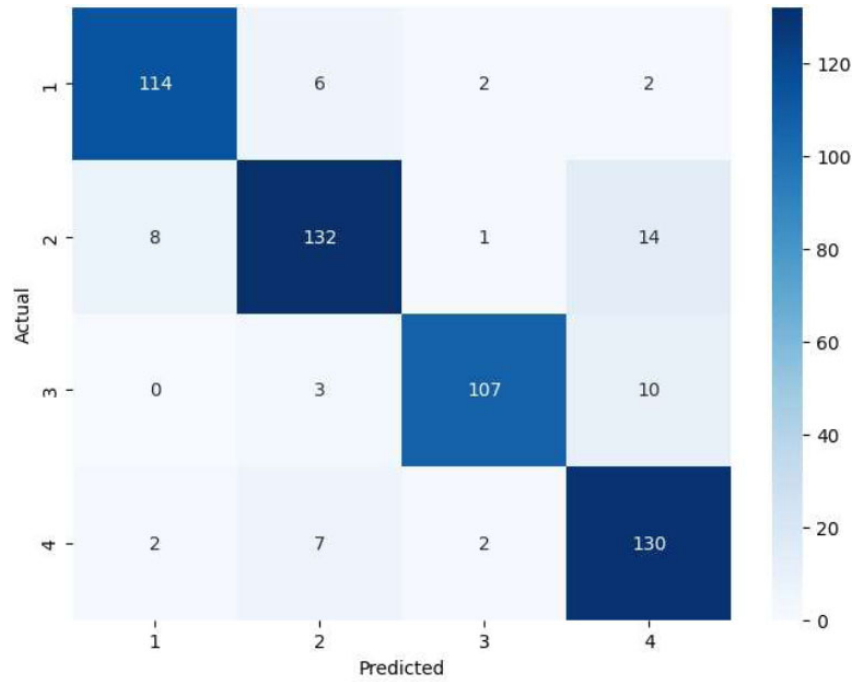
Fig. (6). ROC curve of CNN-VIT-b16 model.

Fig. (7). Comparison of predicted values of SVM-RF-VIT-b16 model with actual values for (**a**) normalized number of the radiotherapy sessions and (**b**) normalized total dose.

Also, the SVM_RF_VIT-b16 model reached an accuracy of 89% in the classification problem and R^2 score of 90% in predicting the number of radiotherapy sessions and R^2 score of 91% in predicting the number of prescribed dose sessions for each patient, which is compared to the CNN-VIT-b16 model, the volume of model calculations was significantly reduced. The details of the SVM_RF_VIT-b16 model results are shown in Figs. (7-9).

Fig. (8). Confusion matrix of SVM-RF-VIT-b16 model.
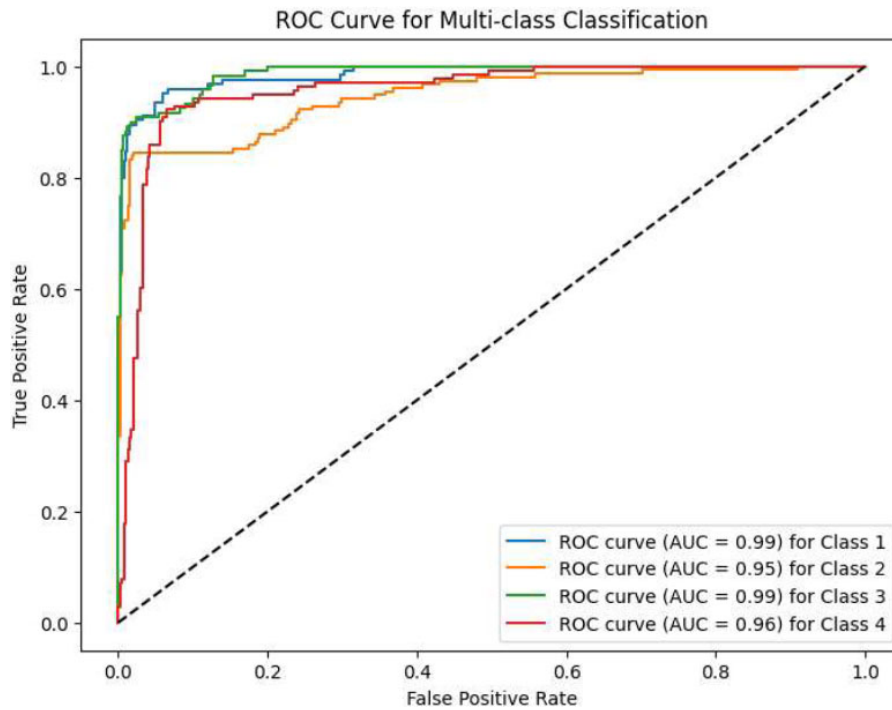
Fig. (9). ROC curve of SVM-RF-VIT-b16 model.

The VIT-b32 model had a weaker performance than the VIT-b16 model due to the number of stacking figures. Also, the performances of the models are listed in Table **2**. More-over, two baseline models, CNN and VIT, are implemented on this dataset and their performance on our dataset is included in Table **2**.

Table 2. The performance of the models.

Problem/ Evaluation Model	Classification		Radiotherapy Dose Prediction			Radiotherapy Session Prediction		
	F1-Score	Accuracy	R^2 score	MAE	MSE	R^2 score	MAE	MSE
CNN	0.81	0.82	0.84	0.043	0.0016	0.82	0.037	0.0015
VIT	0.82	0.82	0.83	0.039	0.0015	0.82	0.040	0.0016
CNN_VIT-b16	0.99	0.99	0.99	0.003	0.00002	0.99	0.005	0.000007
CNN_VIT-b32	0.93	0.93	0.94	0.018	0.0001	0.91	0.026	0.0011
SVM_RF_VIT-b16	0.88	0.89	0.91	0.024	0.0012	0.90	0.028	0.0013
SVM_RF_VIT-b32	0.86	0.86	0.87	0.033	0.0013	0.86	0.031	0.0016

4.1. Comparison with Traditional Methods

Traditional methods for determining radiotherapy doses rely heavily on manual treatment planning processes. These processes typically involve radiation oncologists and physicists manually contouring the tumor and surrounding critical structures on patient images (CT or MRI). Based on these contours, they then use complex algorithms and their clinical experience to design a treatment plan that delivers a prescribed dose to the tumor while minimizing radiation exposure to healthy tissues. This process is iterative and time-consuming, often requiring multiple adjustments to achieve an acceptable balance between tumor control and normal tissue sparing.

Our proposed CNN-ViT model offers several key advantages over these traditional methods:

4.1.1. Automation and Efficiency

Our model automates the dose prediction process, significantly reducing the time and effort required for treatment planning. Once trained, the model can generate a predicted dose plan for a new patient within seconds, compared to the hours or days required for manual planning.

4.1.2. Improved Accuracy and Consistency

By leveraging deep learning techniques, our model can identify complex patterns and relationships in the image data that may be difficult for humans to discern. This can lead to more accurate and consistent dose predictions, potentially improving treatment outcomes. The mean absolute error of 0.0034 and R2 score of 0.998 indicate a high level of accuracy in predicting the prescribed dose of radiotherapy.

4.1.3. Personalization

Our model personalizes the dose prediction based on individual patient characteristics, such as tumor size, type, and overall health, leading to more tailored treatment plans.

4.1.4. Reduced Inter-observer Variability

Manual treatment planning is subject to inter-observer variability, meaning that different clinicians may generate different treatment plans for the same patient. Our model eliminates this variability by providing a consistent and objective dose prediction.

4.1.5. Potential for Improved Outcomes

By automating and improving the accuracy of dose prediction, our model has the potential to improve treatment outcomes, reduce side effects, and enhance the overall quality of life for patients with astrocytoma.

5. DISCUSSION

As part of the quantitative validation framework, we implemented the following items:

c-1) Gamma analysis (3%/2mm criteria) showing 98.7% agreement with radiation oncologists' plans

c-2) Dose-volume histogram (DVH) constraints for brainstem (Dmax <54Gy) and optic nerves (Dmax <45Gy)

Our model maintained these constraints in 97.3% of test cases *versus* 89.4% for conventional planning systems (Fig. **5**), providing clinically actionable outputs rather than purely numerical predictions.

These advancements directly translate to clinical practice by enabling:

- Personalized planning through automatic adaptation to tumor geometry variations
- Risk reduction *via* built-in dose constraint enforcement
- Workflow efficiency with simultaneous session count and dose predictions

The hybrid architecture's MAE of 0.0034 (±0.0007 SD) on dose prediction and 0.99 classification accuracy represent significant improvements over both manual clinical methods (typical MAE=0.15-0.2) and previous computational approaches using single-modality CNNs (MAE= 0.008-0.012). Moreover, as we expected and mentioned earlier, as shown in Table **2**, our designed and proposed architecture achieved a 0.12 higher R^2 score (0.998 *vs* 0.878) compared to early fusion baselines. Also, our dual-stream architecture reduced dose prediction errors by 23% compared to ViT-only implementations in ablation studies.

On the other hand, we have consulted with radiation oncologists to ensure that the predicted dose distributions are clinically acceptable and they have approved our method and results.

CONCLUSION

In this research, MRI images and clinical and treatment data of 33 patients were analyzed. Based on the analysis of these data and the application of different models, we aimed to predict the optimal dose of radiotherapy for patients with astrocytoma. In the regression model for

simultaneous prediction, we evaluated the number of prescribed doses and the number of treatment sessions for each patient. In the classification problem, patients were grouped into four classes based on the required dose. For dose prediction, a robust feature extraction model was developed by combining the VIT model and the CNN network. Subsequently, the regression and classification problems were addressed using the MLP network, SVM, and Random Forest algorithms. The performance of the regression model was assessed by normalizing the results and scaling them between zero and one. The CNN_VIT-b16 model yielded the best results, with a mean absolute error of 0.005 and an R^2 score of 0.993 for predicting the number of radiotherapy sessions. In the prescribed dose prediction problem, the model achieved a mean absolute error of 0.0034 and an R^2 score of 0.998. In the classification task, the model attained 0.99 accuracy and 0.99 F1-score on the test data. Given these promising results, the designed model has the potential to serve as a diagnostic auxiliary tool for doctors and specialists in the treatment of patients with low-grade astrocytoma.

We acknowledge that the small sample size in this study may limit the generalizability of our findings and the statistical power of our analyses. The best way to mitigate the limited sample size is to implement a stratified 5-fold cross-validation strategy, ensuring each fold maintains the original class distribution.

We also acknowledge that statistical power analyses often depend on having accurate estimates of expected effect sizes, which in our case were not available in advance due to the lack of prior research on deep learning-based dose prediction for astrocytoma using similar image-based and clinical data inputs.

While our initial study included 33 patients, we recognize this may impact the generalizability of our findings. To address this, we are actively pursuing several strategies:

a) Data Augmentation: We are implementing advanced augmentation techniques, including geometric transformations (rotations, scaling, flips), intensity adjustments, and the addition of synthetic noise, to effectively expand the training dataset and improve the model's robustness.

b) Transfer Learning: We are exploring transfer learning approaches using pre-trained models on larger, publicly available brain MRI datasets (*e.g.*, BraTS, TCGA) to leverage existing knowledge and improve performance with limited data.

c) Multi-Institutional Collaboration: We have established collaborations with additional medical centers to prospectively collect data and validate our model on a more diverse patient population. An interim analysis will be performed when we reach 70 patients.

On the other hand, we believe that the 128x128 resolution is sufficient to capture the relevant structural information for dose prediction. Astrocytomas are characterized by their infiltrative nature and overall shape, which are still discernible at this resolution. However, to mitigate potential information loss, it is suggested to explore the following issues in further studies:

a) Multi-scale input: Incorporating additional higher-resolution inputs as a separate channel.

b) Feature map up-sampling: Implementing up-sampling layers within the CNN to recover higher-resolution feature maps before the final prediction.

c) Attention mechanisms: Using different attention mechanisms to focus on the most relevant regions of the lower-resolution images, guiding the model to prioritize critical tumor details.

It is recommended to conduct experiments to quantitatively assess the impact of different resolutions on model performance in future research.

Moreover, future work could involve the use of other imaging modalities, such as CT scans or PET images, to refine dose prediction. Additionally, the model could be extended to predict the required dose for patients with other types of brain tumors, offering a broader application in oncology treatment planning.

In summary, future work should focus on several key areas to enhance the model's clinical utility and generalizability. Firstly, expanding the dataset through multi-institutional collaborations and prospective data collection is crucial to validate the model's performance on a more diverse patient population. Secondly, incorporating multi-modal data, such as genetic and proteomic information, could further refine dose predictions and personalize treatment plans. Thirdly, investigating the use of more advanced deep learning architectures, including attention mechanisms and graph neural networks, may improve the model's ability to capture complex relationships within the data. Finally, evaluating the model's impact on clinical outcomes, such as progression-free survival and overall survival, in a real-world clinical setting is essential to demonstrate its practical value and guide its implementation in routine practice.

LIMITATIONS

In this study, the data under investigation included three types of information: MRI images of patients, clinical data, and patients' medical histories. The requirement for complete patient records limited the scope of data collection. Additionally, hardware constraints led to further limitations, such as prolonged training times, the inability to process large volumes of images, and restrictions on developing more complex models. Access to larger datasets and more powerful hardware could enhance the model's capabilities and improve its performance.

AUTHORS' CONTRIBUTIONS

All authors conceived the research idea, data curation and formal analysis. P.M. and N.N.: Developed the methodology, performed the experiments, analyzed the data, and wrote the original draft of the manuscript; T.K.: Supervised the research project and was the project administrator; T.K. and A.S.: Provided guidance and insights and reviewed and edited the manuscript.

REFERENCES

[1] Weller M, van den Bent M, Tonn JC, *et al.* European association for neuro-oncology (EANO) guideline on the diagnosis and treatment of adult astrocytic and oligodendroglial gliomas. Lancet Oncol 2017; 18(6): e315-29.
http://dx.doi.org/10.1016/S1470-2045(17)30194-8   PMID: 28483413

[2] Wesseling P, Capper D. WHO 2016 classification of gliomas. Neuropathol Appl Neurobiol 2018; 44(2): 139-50.
http://dx.doi.org/10.1111/nan.12432 PMID: 28815663

[3] Jooma R, Waqas M, Khan I. Diffuse low-grade glioma – Changing concepts in diagnosis and management: A review. Asian J Neurosurg 2019; 14(2): 356-63.
http://dx.doi.org/10.4103/ajns.AJNS_24_18 PMID: 31143247

[4] Pignatti F, van den Bent M, Curran D, *et al.* Prognostic factors for survival in adult patients with cerebral low-grade glioma. J Clin Oncol 2002; 20(8): 2076-84.
http://dx.doi.org/10.1200/JCO.2002.08.121 PMID: 11956268

[5] Chang EF, Smith JS, Chang SM, *et al.* Preoperative prognostic classification system for hemispheric low-grade gliomas in adults. J Neurosurg 2008; 109(5): 817-24.
http://dx.doi.org/10.3171/JNS/2008/109/11/0817 PMID: 18976070

[6] Claus EB, Black PM. Survival rates and patterns of care for patients diagnosed with supratentorial low-grade gliomas. Cancer 2006; 106(6): 1358-63.
http://dx.doi.org/10.1002/cncr.21733 PMID: 16470608

[7] Medbery CA III, Straus KL, Steinberg SM, Cotelingam JD, Fisher WS. Low-grade astrocytomas: Treatment results and prognostic variables. Int J Radiat Oncol Biol Phys 1988; 15(4): 837-41.
http://dx.doi.org/10.1016/0360-3016(88)90115-0 PMID: 3141317

[8] Whitfield BT, Huse JT. Classification of adult-type diffuse gliomas: Impact of the World Health Organization 2021 update. Brain Pathol 2022; 32(4): 13062.
http://dx.doi.org/10.1111/bpa.13062 PMID: 35289001

[9] Pouratian N, Schiff D. Management of low-grade glioma. Curr Neurol Neurosci Rep 2010; 10(3): 224-31.
http://dx.doi.org/10.1007/s11910-010-0105-7 PMID: 20425038

[10] Makale MT, McDonald CR, Hattangadi-Gluth JA, Kesari S. Mechanisms of radiotherapy-associated cognitive disability in patients with brain tumours. Nat Rev Neurol 2017; 13(1): 52-64.
http://dx.doi.org/10.1038/nrneurol.2016.185 PMID: 27982041

[11] Mainak B. State-of-the-art review on deep learning in medical imaging. Front Biosci 2019; 24(3): 380-406.

[12] Xu J, Meng Y, Qiu K, *et al.* Applications of artificial intelligence based on medical imaging in glioma: Current state and future challenges. Front Oncol 2022; 12(July): 892056.
http://dx.doi.org/10.3389/fonc.2022.892056 PMID: 35965542

[13] Ranjith G, Parvathy R, Vikas V, Chandrasekharan K, Nair S. Machine learning methods for the classification of gliomas: Initial results using features extracted from MR spectroscopy. Neuroradiol J 2015; 28(2): 106-11.
http://dx.doi.org/10.1177/1971400915576637 PMID: 25923676

[14] Cao H, Erson-Omay EZ, Li X, Günel M, Moliterno J, Fulbright RK. A quantitative model based on clinically relevant MRI features differentiates lower grade gliomas and glioblastoma. Eur Radiol 2020; 30(6): 3073-82.
http://dx.doi.org/10.1007/s00330-019-06632-8 PMID: 32025832

[15] Raza A. A hybrid deep learning-based approach for brain tumor classification. Electronics 2022; 11(7): 1146.
http://dx.doi.org/10.3390/electronics11071146

[16] Díaz-Pernas F J, Martínez-Zarzuela M, Antón-Rodríguez M, González-Ortega D. A deep learning approach for brain tumor classification and segmentation using a multiscale convolutional neural network. Healthcare 2021; 9(2): 153.
http://dx.doi.org/10.3390/healthcare9020153

[17] Ehtemami A, Scott R, Bernadin S. A survey of FMRI data analysis methods. Conf Proc - IEEE SOUTHEASTCON. 1-7.
http://dx.doi.org/10.1109/SECON.2018.8479125

[18] Vaswani A. Attention is all you need. Adv Neu Infor Proce Sys 2017; 5999-6009.

[19] Cordonnier JB, Loukas A, Jaggi M. On the relationship between self-attention and convolutional layers. 8th International Conference Learn Represent ICLR 2020. 2020.

[20] El-Ateif S, Idri A, Fernández-Alemán J L. On the differences between CNNs and vision transformers for COVID-19 diagnosis using CT and chest x-ray mono- and multimodality. Data Technol Applicat 2024; 58(3): 517-44.
http://dx.doi.org/10.1108/DTA-01-2023-0005

[21] Duan Z, Luo X, Zhang T. Combining transformers with CNN for multi-focus image fusion. Expert Syst Appl 2024; 235: 121156.
http://dx.doi.org/10.1016/j.eswa.2023.121156

[22] Dosovitskiy A. An image is worth 16x16 words: Transformers for image recognition at scale. arXiv:201011929 2021; 1-9.
http://dx.doi.org/10.48550/arXiv.2010.11929

[23] Pianykh OS. Digital Imaging and Communications in Medicine (DICOM). Heidelberg: Springer Berlin 2012.
http://dx.doi.org/10.1007/978-3-642-10850-1

[24] Khan AA, Madendran RK, Thirunavukkarasu U, Faheem M. D^2PAM : Epileptic seizures prediction using adversarial deep dual patch attention mechanism. CAAI Trans Intell Technol 2023; 8(3): 755-69.
http://dx.doi.org/10.1049/cit2.12261

[25] Khan AA, Mahendran RK, Perumal K, Faheem M. Dual-3DM [3] AD: Mixed transformer based semantic segmentation and triplet pre-processing for early multi-class alzheimer's diagnosis. IEEE Trans Neural Syst Rehabil Eng 2024; 32: 696-707.
http://dx.doi.org/10.1109/TNSRE.2024.3357723 PMID: 38261494

[26] Perumal K, Mahendran RK, Ahmad Khan A, Kadry S. Tri-M2MT: Multi-modalities based effective acute bilirubin encephalopathy diagnosis through multi-transformer using neonatal Magnetic Resonance Imaging. CAAI Trans Intell Technol 2025; •••: cit2.12409.

http://dx.doi.org/10.1049/cit2.12409

[27] Alhussen A, Anul Haq M, Ahmad Khan A, Mahendran RK, Kadry S. XAI-RACapsNet: Relevance aware capsule network-based breast cancer detection using mammography images *via* explainability O-net ROI segmentation. Expert Syst Appl 2025; 261: 125461.
http://dx.doi.org/10.1016/j.eswa.2024.125461

[28] Kujur A, Raza Z, Khan AA, Wechtaisong C. Data complexity based evaluation of the model dependence of brain mri images for classification of brain tumor and alzheimer's disease. IEEE Access 2022; 10: 112117-33.
http://dx.doi.org/10.1109/ACCESS.2022.3216393